Inorganic Chemistry

Communication

pubs.acs.org/IC

An Unprecedented Fe_{36} Phosphonate Cage

Christine M. Beavers,[†] Andrey V. Prosverin,[‡] John D. Cashion,[§] Kim R. Dunbar,*[,‡] and Anne F. Richards*[,⊥]

[⊥]Department of Chemistry, La Trobe Institute for Molecular Sciences, Melbourne, Australia 3086

[†]Advanced Light Source, Lawrence Berkeley National Laboratory, 1 Cyclotron Road, MS15R217, Berkeley, California 94720, United States

[‡]Department of Chemistry, Texas A&M University, College Station, Texas 77842, United States

[§]School of Physics, Monash University, Melbourne, Australia 3800

Supporting Information

ABSTRACT: The reaction of 2-pyridylphosphonic acid (LH_2) with iron(II) perchlorate and iron(III) nitrate afforded an interconnected, double-layered, cationic iron cage, $[\{Fe_{36}L_{44}(H_2O)_{48}\}]^{20+}$ (**1a**), the largest interconnected, polynuclear ferric cage reported to date. Magnetic studies on **1a** revealed antiferromagnetic coupling between the spins on adjacent Fe^{III} ions.

Owing to their relevance in biological systems,[1] their potential as molecular nanomagnets,[2] and the additional benefit of aesthetically pleasing structures, the synthesis of polynuclear cages has become an active field of research over the past few decades.[1−3] Polynuclear ferric complexes are highly desirable synthetic targets because of their relevance to heme proteins and their potential magnetic applications. To date, most of the structurally characterized polynuclear iron cages possess carboxylate ligands.[4] In recent years, several research groups have demonstrated that phosphonic acids are excellent ligands for the stabilization of polynuclear cages.[5−8] Various methods have been employed for the synthesis of molecular cages including the introduction of a second ancillary ligand or use of small preformed cages as starting materials. These strategies have led to a number of iron phosphonate cages containing from 3 to 18 iron atoms.[5−7] Herein we report the reproducible syntheses, structures, and magnetic properties of two polynuclear iron phosphonate cages, **1a** and **1b**, $[\{Fe_{36}L_{44}(H_2O)_{48}\}]^{20+}$ (L = 2-pyridylphosphonate), *differing only in their counteranions*, for **1a** nitrates and perchlorates and for **1b** triflate ions (Figure 1). This is the highest-nuclearity, interconnected, discrete iron cage, i.e., not chains of Fe_n units, reported to date. The unique cage features 36 iron centers and 48 terminal oxygen atoms supported by 44 phosphonate groups with 8 corner-bridging and 36 edge-bridging phosphonate groups with pyridyl interactions to the iron centers. These molecules can be considered iron nanocages because their dimensions are ∼1.3 × 1.5 nm, with an internal diameter of ∼2 nm (from corner to corner).

The room temperature reaction of iron(II) perchlorate and iron(III) nitrate with 2-pyridylphosphonic acid (LH_2) afforded $[\{Fe_{36}L_{44}(H_2O)_{48}\}](ClO_4)_{2.1}(NO_3)_{11.9}(OH)_6\cdot 47.9H_2O\cdot\cdot 10EtOH$ (**1a**). To demonstrate the unequivocal nature of the cationic core, cage $[Fe_{36}L_{44}(H_2O)_{48}](OH)_6(CF_3SO_3)_{14}\cdot\cdot 2EtOH\cdot 72H_2O$ (**1b**) was prepared from the reaction of LH_2 with iron(II) chloride and silver triflate in ethanol/water. It appears that the reaction conditions and the role of the anion play a critical role in determining the final structural motif of

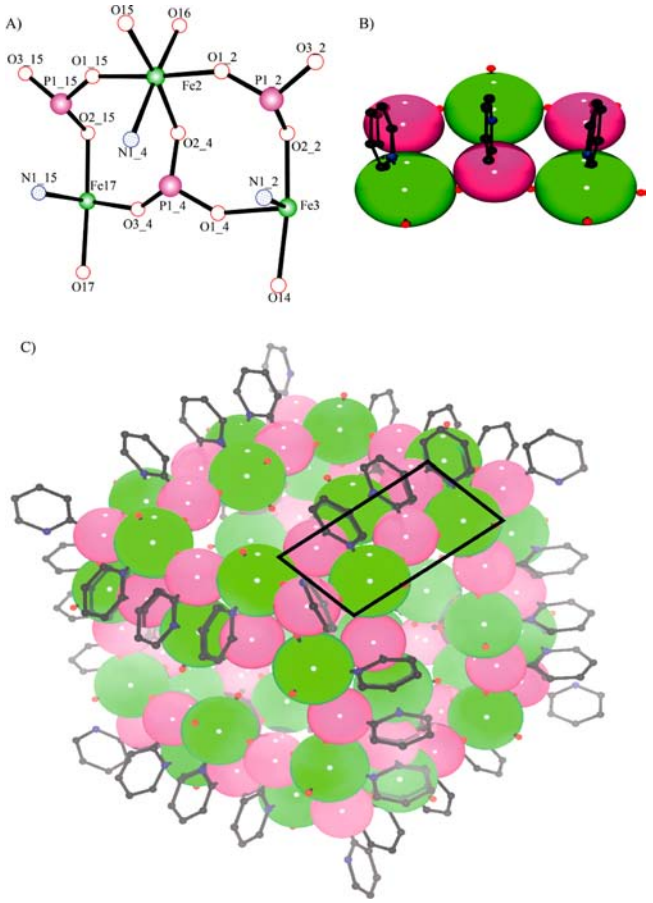

Figure 1. (A) Repeating edge unit in the cage, depicted as coordination spheres (B). (C) Model of the molecular structure of **1a** with coordination spheres emphasized for clarity (solvent molecules and anions are omitted for the sake of clarity). Color code: Fe, green; P, pink; O, red; N, blue; C, gray.

Received: September 16, 2012
Published: January 25, 2013

   dx.doi.org/10.1021/ic3020145 | *Inorg. Chem.* 2013, 52, 1670−1672

these iron cages. The individual reactions of LH_2 with iron(II) perchlorate or iron(III) nitrate yield a previously observed $\{Fe_4L_4\}$ cage[8b] and an amorphous powder, respectively. Ongoing experimental studies have shown that the deployment of mixed-metal precursors, particularly a combination of nitrates and perchlorate salts, yields crystalline molecular cages of various sizes.[8] Nevertheless, this simplistic self-assembly route is sensitive to solvent choice and concentration, requiring a 90:10 mixture of ethanol/water for the preparation of **1a**. Obtaining crystals of **1a** and **1b** requires a slow evaporation of the solvent and isolation of the crystalline material before formation of an insoluble precipitate. This method results in a low, but highly reproducible yield of pure crystalline material. If the solution is left to evaporate further, a powder precipitate forms that is not representative of the crystalline product and is a mixture of iron oxides, hydroxides, and various perchlorate salts. The isolated crystals, when stored under ambient conditions, are found to be very hygroscopic, forming an oily material, but under an inert atmosphere, crystallinity is retained. It is interesting to note that crystals of **1a** and **1b** are almost colorless, arising from pale-yellow solutions. Iron(III) complexes can be a variety of colors, with the more intense colors generally arising from charge transfer. Colorless iron(III) complexes are known,[9] including those containing phosphonate ligands,[9c] and are more likely for high-spin d^5 complexes with spin-forbidden d−d transitions and charge transfer occurring in the far-visible/near-UV region.[9]

Complex **1a** crystallizes in the monoclinic space group $C2/c$, with half of the cation (18 iron atoms and 22 ligands) in the asymmetric unit. The cationic core (iron phosphonate units) has nearly O_h symmetry. Inclusion of the ligands reduces the symmetry, to more closely approximate T. The cage symmetry is also conducive to crystallization in trigonal space groups, as evidenced by complex **1b** crystallizing in the rhombohedral space group $R\bar{3}c$ in a hexagonal setting. In **1a**, the cage is generated by a crystallographic inversion center ($^1/_2$, 0, $^1/_2$), whereas in **1b**, the cage is generated by $a\bar{3}$.[10] Disorder of the interstitial molecules in crystals is a common feature of large polynuclear cages and host−guest complexes that contain large void spaces in which disordered solvent or counterions can reside.[11] In this case, we have crystallization of nanocages over hundreds of micrometers; this amount of long-range order is impressive; but, the diffuse scattering and poor mosaicity resulting from loose association between the discrete molecules result in extremely difficult crystallography. However, as shown by Dahl and co-workers and Colquhoun et al.,[12] poorly diffracting crystals can lead to invaluable structural information, in this case the clear discrimination of the $\{Fe_{36}L_{44}\}$ cage formed by two independent routes with different anions. Despite the crystallographic disorder of the solvent and anions, the atom connectivity and topology of the two identical iron cages is unambiguous and is clearly the most important part of the crystal structures. A detailed description of the refinement process for both cages is provided in the Supporting Information.

The molecular structure of the cationic cage features a dual-shell arrangement in which 36 octahedrally coordinated iron centers are connected by tetrahedral phosphonate ligands in a 3.111 bridging mode (Harris notation).[13] The metric parameters of the molecular cage exhibit Fe−O bond lengths indicative of Fe^{III} centers. Two distinct iron layers can be observed where the outer (edge)-shell iron atoms have four of the six available coordination sites occupied by phosphonate oxygen atoms and a dative bond to the pyridyl nitrogen atom, with the remaining site occupied by a water molecule. The inner (face) iron atoms have three sites occupied by phosphonate oxygen atoms, a pyridyl nitrogen atom, and two water molecules. With the exception of the eight corners of the cage, the pyridyl nitrogen atoms participate in bonding to the iron atoms. The overall topology of the cage is such that the inner and outer shells alternate between octahedral iron centers and phosphonate groups; for example, in the outer shell, the linkage of Fe−P−Fe would be P−Fe−P in the inner shell. This arrangement leads to an eight-membered building block of Fe−O−P units (Figure 1A).

The structure of $\{Fe_{36}L_{44}\}$ is quite different from the majority of reported polynuclear iron phosphonate cages. Many iron phosphonate cages feature a butterfly arrangement or are based on a triangular arrangement of interconnected iron atoms, affording dense molecular, single-stranded cages.[2−7] By comparison, $\{Fe_{36}L_{44}\}$ is more similar to the single-stranded ferric wheel-type structures,[14] such as the ferric square, $[Fe_{12}]^{8+}$ supported by propanediol and 2,2′:6′2″-terpyridine,[15] and an Fe_{16} complex, $[Fe_{16}(EtO)_4(O_2CPh)_{16}(Hthme)_{12}](NO_3)_4$ [H_3thme = 1,1,1-tris(hydroxymethyl)ethane].[16] Both of these complexes exhibit antiferromagnetic exchange interactions between the iron atoms. While ferric wheels as large as Fe_{64} and Fe_{168} have been reported,[17,18] these architectures differ enormously from $\{Fe_{36}L_{44}\}$, which are assembled by the connection of lower-dimensionality aggregates by a multitopic ligand. For example, the Fe_{168} cage consists of six homochiral wheel-like $\{Fe_{28}\}$ building blocks rather than an interconnected iron network.[18]

Evidence for the oxidation states and environments of the iron centers was provided by various spectroscopic techniques (see the SI). Most relevant is the room temperature Mössbauer spectrum of **1a**, which exhibits a quadrupole doublet (see the SI). The isomer shifts are 0.41(1) mm·s^{-1} for the more intense inner doublet and 0.40(1) mm·s^{-1} for the outer doublet. These values are in excellent agreement with the isomer shifts of other ferric wheel materials.[19] The quadrupole splittings are 0.39(1) and 1.02(2) mm·s^{-1}, respectively, and are within the range expected for ferric iron. The area ratio of the two subspectra is 65:35, suggestive of a 2:1 ratio of two iron sites (inner and outer), with the less intense one being more distorted.

Additionally, the solid-state direct-current magnetic properties of a polycrystalline sample of compound **1a** were measured in the 2−280 K temperature range in an applied magnetic field of 5000 G. The room temperature χT value is 126 emu·mol^{-1}·K^{-1}, which is less than the expected value for 36 uncoupled Fe^{III} ions ($S = {}^5/_2$, g = 2.0, and χT = 157.5 emu·mol^{-1}·K^{-1}). The χT value continuously decreases from the value at room temperature and reaches a minimum of 4.4 emu·mol^{-1}·K^{-1} at 2 K. The temperature dependence of $1/\chi$ in the temperature range 20−280 K approximates Curie−Weiss behavior with C = 158 emu·mol^{-1}·K^{-1} and $\theta = -65$ K. The negative Curie−Weiss constant and the reduced room temperature χT value indicates overall antiferromagnetic interactions between Fe^{III} ions. The obtained magnetic data are similar to those of other iron(III) phosphonate systems.[20] The redox properties of **1a** were investigated by cyclic voltammetry in solution and the solid phase and were found to be electrochemically silent.

In conclusion, a nanosized polynuclear iron cage containing 36 iron centers has been prepared, a result that underscores the

dx.doi.org/10.1021/ic3020145 | Inorg. Chem. 2013, 52, 1670−1672

versatility of phosphonic acids for the preparation of novel and potentially technologically useful materials.

■ ASSOCIATED CONTENT

Supporting Information

X-ray crystallographic data in CIF format, experimental details, crystal data, and spectroscopic data. This material is available free of charge via the Internet at http://pubs.acs.org.

■ AUTHOR INFORMATION

Corresponding Author

*E-mail: a.richards@latrobe.edu.au (A.F.R.), dunbar@mail.chem.tamu.edu (K.R.D.).

Notes

The authors declare no competing financial interest.

■ ACKNOWLEDGMENTS

A.F.R. acknowledges the ARC for the award of a Future Fellowship (Grant FT100100003). K.R.D. gratefully acknowledges the DOE (Grant DE-FG02-02ER45999) and the NSF for a grant to purchase a SQUID magnetometer (Grant NSF-9974899). The Advanced Light Source is supported by the Director, Office of Science, Office of Basic Energy Sciences, DOE, under Contract DE-AC02-05CH11231.

■ REFERENCES

(1) For example, see: (a) Taft, K. L.; Papaefthymiou, G. C.; Lippard, S. J. *Science* **1993**, *259*, 1302−1305. (b) Theil, E. C.; Matzapetakis, M.; Liu, X. J. *J. Biol. Inorg. Chem.* **2006**, *11*, 803−810. (c) Lee, S. C.; Holm, R. H. *Chem. Rev.* **2004**, *104*, 1135−1158.

(2) (a) Chesman, A. S. R.; Turner, D. R.; Moubaraki, B.; Murray, K. S.; Deacon, G. B.; Batten, S. R. *Dalton Trans.* **2012**, *41*, 3751−3757. (b) Powell, G. W.; Lancashire, H. N.; Brechin, E. K.; Collison, D.; Heath, S. L.; Mallah, T.; Wernsdorfer, W. *Angew. Chem., Int. Ed.* **2004**, *43*, 5772−5775.

(3) Tasiopoulos, A. J.; Vinslava, A.; Wernsdorfer, W.; Abboud, K. A.; Christou, G. *Angew. Chem., Int. Ed.* **2004**, *43*, 2117−2121.

(4) (a) Goodwin, J. C.; Sessoli, R.; Gatteschi, D.; Wernsdorfer, W.; Powell, A. K.; Heath, S. L. *J. Chem. Soc., Dalton Trans.* **2000**, 1835−1840. (b) Abu-Nawwas, A.-A. H.; Mason, P. V.; Milway, V. A.; Muryn, C. A.; Pritchard, R. J.; Tuna, F.; Collison, D.; Winpenny, R. E. P. *Dalton Trans.* **2008**, *2*, 198−200.

(5) (a) Tolis, E. I.; Helliwell, M.; Langley, S.; Raftery, J.; Winpenny, R. E. P. *Angew. Chem., Int. Ed.* **2003**, *42*, 3804−3808. (b) Khanra, S.; Konar, A.; Clearfield, A.; Helliwell, M.; McInnes, E. J. L.; Tolis, E.; Tuna, F.; Winpenny, R. E. P. *Inorg. Chem.* **2009**, *48*, 5338−5349. (c) Konar, S.; Bhuvanesh, N.; Clearfield, A. *J. Am. Chem. Soc.* **2006**, *128*, 9604−9605.

(6) Khanra, S.; Helliwell, M.; Tuna, F.; McInnes, E. J. L.; Winpenny, R. E. P. *Dalton Trans.* **2009**, 6166−6174.

(7) (a) Konar, S.; Clearfield, A. *Inorg. Chem.* **2008**, 5573−5579. (b) Tolis, E. I.; Engelhardt, L. P.; Mason, P. V.; Rajaraman, G.; Kindo, K.; Luban, M.; Matsuo, A.; Nojiri, H.; Raftery, J.; Schröder, C.; Timco, A.; Tuna, F.; Wernsdorfer, W.; Winpenny, R. E. P. *Chem.—Eur. J.* **2006**, *12*, 8961−8968. (c) Mitkina, T. V.; Lan, Y.; Mereacre, V.; Shi, W.; Powell, A. K.; Rothenberger, A. *Dalton Trans.* **2008**, 1136−1139.

(8) (a) Samanamu, C. R.; Olmstead, M. M.; Montchamp, J.-L.; Richards, A. F. *Inorg. Chem.* **2008**, *47*, 3879−3887. (b) Zavras, A.; Fry, J. A.; Beavers, C. M.; Richards, A. F. *CrystEngComm* **2011**, *13*, 3551−3561.

(9) Examples include the following: (a) Abu-Shandi, K.; Winkler, H.; Wu, B.; Janiak, C. *CrystEngComm* **2003**, *5*, 180−180. (b) Zima, V.; Kwang-Hwa, L. *J. Chem. Soc., Dalton Trans.* **1998**, 4109−4112. (c) Du, Z.-Y.; Sun, Y.-H.; Liu, Q.-Y.; Xie, Y.-R.; Wen, H. R. *Inorg. Chem.* **2009**, *48*, 7015−7017.

(10) Crystal data for **1a**: $[Fe_{36}L_{44}(H_2O)_{48}](ClO_4)_{2.1}(NO_3)_{11.9}(OH)_6{\cdot}47.9H_2O{\cdot}10EtOH$, colorless block, monoclinic, $C2/c$, a = 43.6079(17) Å, b = 28.7572(10) Å, c = 50.5916(19) Å, β = 120.999(2)°, V = 54383(3) Å^3, T = 150(2) K, λ =1.03320 Å, Z = 4, R1 [$I > 2\sigma(I)$] = 0.1927, wR2 (all data) = 0.5115, GOF (on F^2) = 3.750. Crystal data for **1b**: $[Fe_{36}L_{44}(H_2O)_{48}](OH)_6(CF_3SO_3)_{14}{\cdot}2EtOH{\cdot}72H_2O$, colorless block, trigonal, $R\bar{3}c$, a = 28.6989(3) Å, c = 132.1838(12) Å, V = 94284.3(16) Å^3, T = 130(2) K, Z = 6, R1 [$I > 2\sigma(I)$] = 0.1480, wR2 (all data) = 0.4606, GOF (on F^2) = 2.156.

(11) (a) Ko, Y. H.; Kim, K.; Kang, J.-K.; Chun, H.; Lee, J. W.; Sakamoto, S.; Yamaguchi, K.; Fettinger, J. C.; Kim, K. *J. Am. Chem. Soc.* **2004**, *126*, 1932. (b) Johnson, D. W.; Xu, J.; Saalfrank, R. W.; Raymond, K. N. *Angew. Chem., Int. Ed.* **1999**, *38*, 2882. (c) Içli, B. A.; Christinat, N.; Tönnemann, J.; Schüttler, C.; Scopelliti, R.; Severin, K. *J. Am. Chem. Soc.* **2009**, *131*, 3154.

(12) (a) Mednikov, E. G.; Ivanov, S. A.; Slovokhotova, I. V.; Dahl, L. F. *Angew. Chem., Int. Ed.* **2005**, *44*, 6848. (b) Zhu, Z.; Cardin, C. J.; Gan, Y.; Colquhoun, H. M. *Nat. Chem.* **2010**, *2*, 653.

(13) Coxall, R. A.; Harris, S. G.; Henderson, D. K.; Parsons, S.; Tasker, P. A.; Winpenny, R. E. P. *Dalton Trans.* **2000**, 2349−2356.

(14) Taft, K. L.; Lippard, S. J. *J. Am. Chem. Soc.* **1990**, *112*, 9629−9630.

(15) Stamatatos, T. C.; Christou, A. G.; Jones, C. M.; O'Callaghan, B. J.; Abboud, K. A.; O'Brien, T. A.; Christou, G. *J. Am. Chem. Soc.* **2007**, *129*, 9840−9841.

(16) Jones, L. J.; Low, D. M.; Helliwell, M.; Raftery, J.; Collison, D.; Aromí, G.; Cano, J.; Mallah, T.; Wernsdorfer, W.; Brechin, E. K.; Mcinnes, E. J. L. *Polyhedron* **2006**, *25*, 325−333.

(17) Liu, T.; Zhang, Y.-J.; Wang, Z.-M.; Gao, S. *J. Am. Chem. Soc.* **2008**, *130*, 10500−10501.

(18) Zhang, Z.-M.; Yao, S.; Li, Y.-G.; Clérac, R.; Lu, Y.; Su, Z.-M.; Wang, E.-B. *J. Am. Chem. Soc.* **2009**, *131*, 14600−14601.

(19) (a) Zhang, Z.-M.; Li, Y.-G.; Yao, S.; Wang, E.-B.; Wang, Y.-H.; Clerac, R. *Angew. Chem., Int. Ed.* **2009**, *48*, 1581−1584. (b) Raptopoulou, C. P.; Tangoulis, V.; Devlin, E. *Angew. Chem., Int. Ed.* **2002**, *41*, 2386−2389.

(20) (a) Khanra, S.; Konar, A.; Clearfield, A.; Helliwell, M.; McInnes, E. J. L.; Tolis, E.; Tuna, F.; Winpenny, R. E. P. *Inorg. Chem.* **2009**, *48*, 5338−5349. (b) Gopal, K.; Tuna, R.; Winpenny, R. *Dalton Trans.* **2011**, *40*, 12044−12047. (c) Song, H. H.; Zheng, L.-M.; Zhu, G.; Shi, Z.; Feng, S.; Gao, S.; Hu, Z.; Xin, X.-Q. *J. Solid State Chem.* **2002**, *164*, 367−373. (d) Zhang, Z.-C.; Bao, S.-S.; Zheng, L.-M. *Inorg. Chem. Commun.* **2007**, *10*, 1063−1066.